Probing Localization in Absorbing Systems via Loschmidt Echos

Joshua D. Bodyfelt,[1] Mei C. Zheng,[1,2] Tsampikos Kottos,[1,2] Ulrich Kuhl,[3] and Hans-Jürgen Stöckmann[3]

[1]*Department of Physics, Wesleyan University, Middletown, Connecticut 06459, USA*

[2]*MPI for Dynamics and Self-Organization—Bunsenstraße 10, D-37073 Göttingen, Germany*

[3]*Fachbereich Physik, Philipps-Universität Marburg, Renthof 5, D-35032 Marburg, Germany*

(Received 28 January 2009; published 23 June 2009)

We measure Anderson localization in quasi-one-dimensional waveguides in the presence of absorption by analyzing the echo dynamics due to small perturbations. We specifically show that the inverse participation number of localized modes dictates the decay of the Loschmidt echo, differing from the Gaussian decay expected for diffusive or chaotic systems. Our theory, based on a random matrix modeling, agrees perfectly with scattering echo measurements on a quasi-one-dimensional microwave cavity filled with randomly distributed scatterers.

DOI: 10.1103/PhysRevLett.102.253901 PACS numbers: 42.25.Dd, 03.65.Nk, 03.65.Yz, 72.15.Rn

The propagation of waves through complex media is an interdisciplinary problem that addresses areas as diverse as light propagation in fog or clouds, to electronic and atomic-matter waves used to transmit energy and information. Despite this diversity, the wave character of these systems provides a common framework for understanding their transport properties and often leads to new applications. One such characteristic is a wave interference phenomenon. Its existence results in a complete halt of wave propagation in random media which can be achieved by increasing the randomness of the medium. This phenomenon was predicted 50 years ago in the framework of quantum (electronic) waves by Anderson [1,2] and since then has developed as a field of its own.

Despite the enormous research efforts by various groups in measuring Anderson localization, it took nearly 40 years to observe localization phenomena beyond any doubt. A decisive step towards this direction was done by optics and microwave experiments which allow a detailed study of the Anderson localization, undisturbed by interactions or other effects which characterize electron propagations. First experiments showing photon localization [3] had the problem of separating localization from absorption, which can be another source of exponential decay of a propagating electromagnetic wave. A solution to this problem was given by Chabanov *et al.* in Ref. [4], where they proposed to study the relative size of fluctuations of certain transmission quantities. They found clear evidence of localization in a quasi-one-dimensional (1D) microwave waveguide with randomly distributed dielectric or metallic spheres [4] (see also Fig. 1).

This approach, although quite powerful, does not allow the view of transport from a dynamical perspective, nor makes a direct contact with the original ideas of Anderson theory, which suggests probing localization by means of the sensitivity of the system properties against small perturbations [5]. This approach led us in recent years to focus on new measures that efficiently probe the complexity of quantum time evolution. One such measure is the so-called Loschmidt echo (LE), or fidelity, which probes the sensitivity of quantum dynamics to external perturbations (for review, see Ref. [6]). The recent literature on the subject is vast and ranges from atomic physics [7], microwaves [8], elastic waves [9] to quantum information [10], and quantum chaos [11–15]. Formally, the LE $F^{\lambda}(t)$, is defined as [8]

$$F^{\lambda}(t) \equiv |f^{\lambda}(t)|^2 = |\langle \psi_0 | e^{iH_0 t/\hbar} e^{-iH_\lambda t/\hbar} | \psi_0 \rangle|^2; \quad (1)$$

where $f^{\lambda}(t)$ is the fidelity amplitude, $H_\lambda = H_0 + \lambda V$ is a one-parameter family of Hamiltonians, H_0 is the unperturbed Hamiltonian, λV, where $\langle |V_{nm}|^2 \rangle = 1$, represents a perturbation of strength λ, and $|\psi_0\rangle$ is an initial state.

Fidelity in its original definition, Eq. (1), is hardly accessible to any experiment where the information about

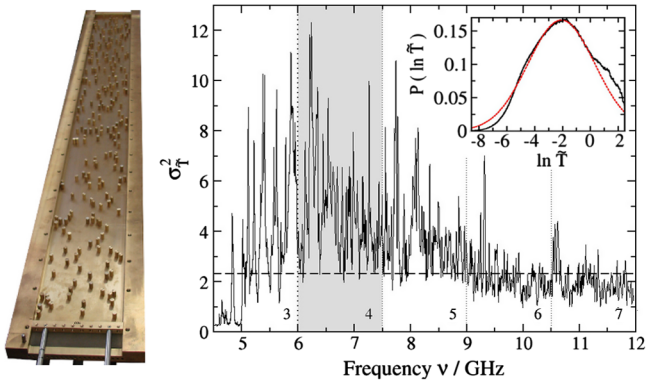

FIG. 1 (color online). Left: Experimental setup—the top plate with two mounted antennae has been removed to show the waveguide with scatterers. Right: The variance of the normalized transmission intensity $\tilde{T} = |S_{21}|^2/\langle |S_{21}|^2 \rangle$. Vertical dashed lines are the mode cutoff frequencies. The numbers between are the number of open modes. The horizontal dashed line is the localization threshold of 7/3. The shaded region is a localized frequency window of 6.0–7.5 GHz. Inset: Transmission distribution $\mathcal{P}(\tilde{T})$ for the localized frequency window of 6.0–7.5 GHz. The red dashed line is a fit ($\chi^2 = 0.094$) of the core to a log-normal distribution, with a width of $\sigma^2_{\tilde{T}} = 3.37$.

the system's state is based on the measurements of certain observables; the most popular being the scattering matrix itself. Therefore, the notion of scattering fidelity had been introduced as an alternative to Eq. (1) [16]. In fact, it was shown that under certain conditions the scattering fidelity coincides with the standard fidelity [16].

We present here the first measurements of fidelity of localized waves. Using a quasi-1D disordered cavity in the localized regime (see left of Fig. 1), we investigate the fidelity decay of microwave radiation, due to small perturbations λ in the form of boundary displacements of the sample, and find deviations from a Gaussian decay expected in a frequency interval associated with extended waves. Using a banded random matrix (BRM) theory modeling, we find that the fidelity amplitude decays as:

$$f(t) \simeq (\alpha t)^2 \mathrm{csch}^2(\alpha t); \qquad \alpha = \lambda\sqrt{1.5 I_2}, \tag{2}$$

where $I_2 = \int |\psi(\mathbf{r})|^4 d\mathbf{r} \propto 1/l_\infty$ is the inverse participation number (IPN), inversely proportional to the localization length. Using a scaling analysis of α with respect to λ we extract I_2 and measure the localization properties of the sample, *even if absorption is present*. Our theoretical results, Eq. (2), are confirmed by our experimental measurements of scattering fidelity.

The scattering fidelity amplitude is defined as

$$f_{ab}^{\lambda}(t) = \langle S_{ab}^{\lambda *}(t) S_{ab}^{0}(t)\rangle / \sqrt{\langle |S_{ab}^{\lambda}(t)|^2\rangle \langle |S_{ab}^{0}(t)|^2\rangle}, \tag{3}$$

where $S_{ab}(t)$ is one component of the scattering matrix in the time domain, while the indices a and b refer to the antennae involved. In microwave studies the S_{ab} are directly accessible from transmission or (for $a = b$) reflection measurements in the frequency domain. The corresponding quantities in the time domain are obtained by Fourier transforms. The superindices λ, 0 indicate scattering matrix elements corresponding to the perturbed and unperturbed system, respectively. The denominator in Eq. (3) renormalizes the fidelity decay due to absorption, thus allowing us to trace out localization phenomena [16]. This assumes a global decay of the scattering matrix elements due to absorption, and no correlation between absorption and scattering. The technique is equivalent to the one adopted in [4] to get rid of absorption.

The experiment has been performed in a quasi-1D rectangular waveguide (height 8 mm, width 100 mm, length 1190 mm) containing 186 randomly distributed brass cylinders of radius 5 mm (see left of Fig. 1). One end of the waveguide holds a fixed reflecting metallic wall, while at the other end there is a moveable reflecting metallic wall, which can be adjusted by means of a step motor. One antenna was placed close to the moving wall, while another one was placed in the center of the scattering arrangement. Measurements have been performed in the frequency range 3 to 12 GHz. The cutoff frequency for the lowest mode is 1.5 GHz, while at the upper limit of the studied frequency range there are 7 propagating modes. The reflection amplitude at the center antenna (S_{22}) and the transmission amplitudes between the two antennae (S_{21}) have been measured for different wall positions. The reflection amplitude S_{22} is used in Eq. (3), and the transmission amplitudes S_{21} are used in transmissive studies below. The wall shift has been performed in steps of $\delta w = 0.2$ mm up to a total shift of 18 mm. In addition, an ensemble average over 15 different realizations of scatterer positions has been performed.

In order to get confidence that our analysis is performed within the appropriate frequency window where localization is present, we first investigate the variance $\sigma_{\tilde{T}}^2$ of the normalized transmission intensity $\tilde{T} = |S_{21}|^2/\langle |S_{21}|^2\rangle$ [4]. Since our experiment does not probe the total transmission but just one component of the scattering matrix, we expect localization whenever $\sigma_{\tilde{T}}^2$ exceeds the critical value of $7/3$ [4]. We find (see Fig. 1) that this condition is satisfied approximately in the frequency window 5.5–9 GHz. Above 9 GHz the waveguide modes are delocalized, while below 5.5 GHz the values of the variances are error prone, as S_{21} is below the precision of the vector network analyzer ($|S_{21}| < 10^{-6}$). In the delocalized regime, random matrix theory predictions are applicable [17], yielding a value of $\sigma_{\tilde{T}}^2 = (2N+1)^2/[N(2N+3)] - 1$, where N is the number of open channels. In the limit $N \to \infty$, the variance approaches the value $\sigma_{\tilde{T}}^2 = 1$, in agreement with our experimental data showing in the high frequency regime values between 1 and 2 for $\sigma_{\tilde{T}}^2$ (see Fig. 1).

We have also investigated the whole normalized transmission distribution $\mathcal{P}(\tilde{T})$. As expected [18], we find a transition from a Rayleigh-like behavior (applicable in the delocalized regime) to a broader distribution approaching a log-normal behavior deep in the localized regime (see inset of Fig. 1 showing $\mathcal{P}(\tilde{T})$ in the localized frequency window of 6–7.5 GHz.).

Next, we measure the scattering fidelity in the localized frequency window (see previous analysis), and compare the experimental data with the LE decay law found for chaotic or diffusive systems [6,8]. The latter reads

$$F(t) \simeq e^{-\lambda^2 \mathcal{C}(t)}; \quad \mathcal{C}(t) \equiv t^2 + t - \int_0^t d\tau \int_0^\tau d\tau' b_2(\tau'), \tag{4}$$

which for small perturbations can be approximated as $F(t) \sim \exp(-(\lambda t)^2)$. Above, b_2 is the two-point form factor for the Gaussian orthogonal ensemble [6]. Using λ as a fitting parameter, we have attempted to fit the experimental data with Eq. (4). We found that the overall agreement is poor (see Fig. 2). Further analysis (see below) confirms that Eq. (4) is inapplicable in the localized regime. On the contrary, when fitting the experimental data with Eq. (2) we get an excellent agreement.

The analytical calculation of $f(t)$ relies on the relation between scattering fidelity and the LE in the weak coupling regime where our experiment operates. The LE was further evaluated using a random matrix theory modeling for H_0 and V. For diffusive or chaotic cavities, H_0 and V are modeled by matrices drawn from a Gaussian orthogonal ensemble (GOE). Anderson localization in quasi-1D dis-

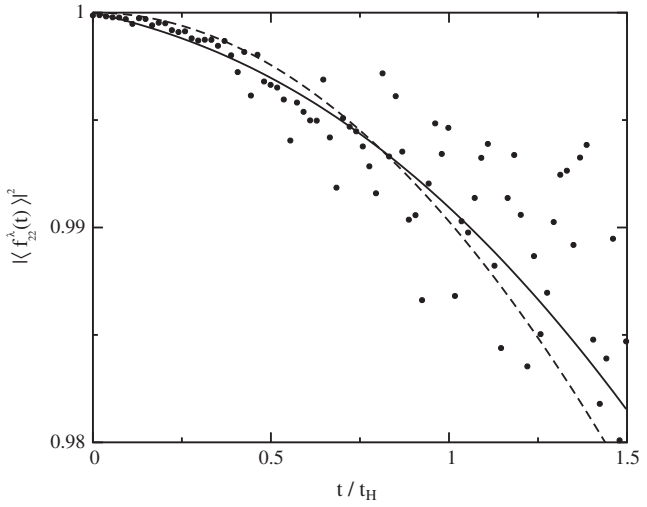

FIG. 2. Experimental scattering fidelity in the frequency window of 6 to 7.5 GHz (localized). The dots correspond to the experimental scattering fidelity, Eq. (3), for a wall shift of 0.8 mm. The dashed line is a best fit to Eq. (4), while the solid line is a best fit to Eq. (2). Both fits were done for the region $t \leq t_H$. Equation (2) can be seen as the better fit.

ordered systems, on the other hand, is modeled by sharp banded GOE matrices with bandwidth b for H_0 and V [19,20]. In this model, the localization length scales as $l_\infty \sim b^2$. Therefore, localization sets in for matrices of rank $L \gg b^2$.

Expanding the initial preparation as $|\psi_0\rangle = \sum_n a_n |\phi_n^0\rangle$, where $H_0|\phi_n^0\rangle = E_n^0|\phi_n^0\rangle$, it is found that the fidelity amplitude defined in Eq. (1) can be written as

$$f(t) = \sum_{n,m,k} \alpha_n^* \alpha_k \langle \phi_m^\lambda | \phi_k^0 \rangle \langle \phi_n^0 | \phi_m^\lambda \rangle e^{-i(E_m^\lambda - E_n^0)t}, \quad (5)$$

where $H_\lambda|\phi_n^\lambda\rangle = E_n^\lambda|\phi_n^\lambda\rangle$. Averaging over disordered realizations one further gets that

$$\overline{f(t)} = \sigma \sum_{n,m} \mathcal{L}_{mn} \exp[-i(E_m^\lambda - E_n^0)t], \quad (6)$$

where $\sigma = \frac{1}{l_\infty} \sum_{n \leq l_\infty} \overline{|\psi_0(n)|^2}$, $\psi_0(n)$ are the components of the initial preparation $|\psi_0\rangle$ in the position basis, and $\mathcal{L}_{mn} = |\langle \phi_m^\lambda | \phi_n^0 \rangle|^2$ is the local density of states kernel [21]. In order to derive Eq. (6) we have assumed statistical independence between the eigenfunctions and eigenvalues of our Hamiltonian, while localization enforces the following contraction rule $\overline{\alpha_n^* \alpha_k} = \sigma \delta_{n,k}$.

For small enough perturbations, such that only nearby (on the order of mean level spacing) energy levels are mixed, one can approximate $\mathcal{L}_{mn}$ in Eq. (6) with a delta function. The fidelity amplitude is then written as

$$\overline{f(t)} \simeq \overline{\sum_n \exp(-i v_n \lambda t)} = \int dv \mathcal{P}(v) \exp(-i v \lambda t), \quad (7)$$

where $v_n = (E_n^\lambda - E_n^0)/\lambda$ are the so-called level velocities, and $\mathcal{P}(v)$ is their corresponding distribution. The latter has been calculated in Ref. [22], and it was found that in the localized regime it is given by the expression

$$P(\eta) = \frac{\pi}{6} \frac{\pi\eta \coth(\pi\eta/\sqrt{6}) - \sqrt{6}}{\sinh^2(\pi\eta/\sqrt{6})}, \quad (8)$$

where $\eta = v/\sigma_v$. For localized level velocities, the variance is $\sigma_v = \sqrt{I_2}$ [23]. Substituting the above distribution in Eq. (7) we finally get the expression given in Eq. (2). The latter is checked numerically for two different bandwidths $b = 10$, 3 and for a system size $L = 5000$. Our numerical results are reported in Fig. 3, together with Eqs. (2) and (4). To confirm further the validity of our calculations, we have fit the decay of the LE for various bandwidths b, with Eq. (2). From the fit we have extracted σ_v, which we have plotted against the IPN I_2, in the inset of Fig. 3. The observed linear behavior gives further confirmation to our theoretical calculations.

We then analyze the decay of scattering fidelity due to small displacements of one wall of the disordered quasi-1D waveguide shown in Fig. 1. The shift of the wall can be mapped onto an effective Hamiltonian H_{λ_w} with matrix elements [16]

$$(H_{\lambda_w})_{nm} = -w \int_0^L \nabla_\perp[\psi_n(y)] \nabla_\perp[\psi_m(y)] dy, \quad (9)$$

where w and L are the shift and length of the moving wall, respectively, and $\nabla_\perp \psi_n$ and $\nabla_\perp \psi_m$ are the normal derivatives of the wave functions at the wall. Thus $\sigma_{\lambda_w} \propto w^2$. The proportionality constant is $(2Lk^3/3\pi^3)$, for the case of chaotic cavities in the semiclassical limit [16]. In any case, we finally get that $\lambda_w \sim w$.

Next we proceed by fitting our experimental data on the scattering fidelity with Eqs. (2) and (4) where α, λ are used

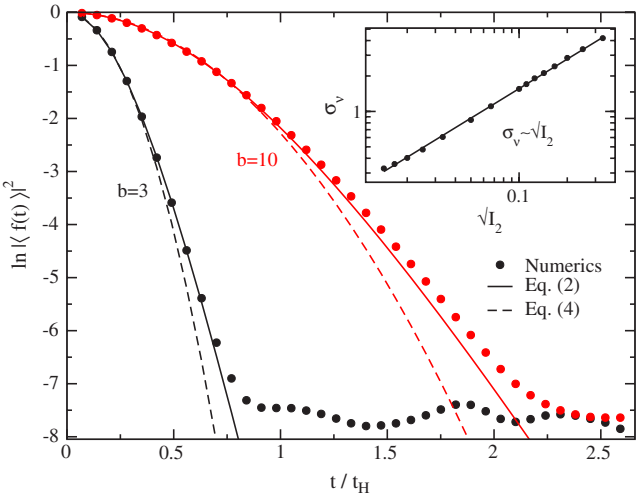

FIG. 3 (color online). Fidelity, Eq. (1), for Hamiltonians modeled by BRM. The parameters are $\lambda = 10^{-3}$, $L = 5000$, $b = 10$ (upper curve), and $b = 3$ (lower curve). Circles are the numerical results. Dashed lines are best fits to Eq. (4). Solid lines are best fits to Eq. (2), which again show a better fit. The inset shows the variance extracted from the fit of Eq. (2), plotted against the root of the inverse participation number. The observed linear relation confirms the validity of Eq. (2).

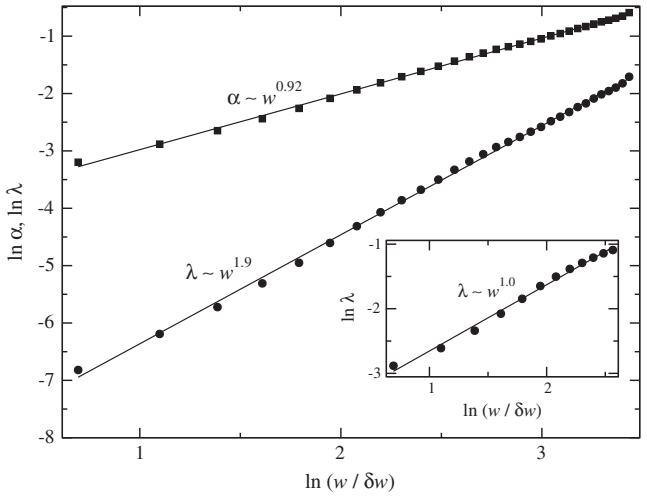

FIG. 4. Within the localized frequency window of 6–7.5 GHz, the experimental fitting parameters—α (squares) from Eq. (2) and λ (circles) from Eq. (4)—are plotted against the rescaled wall shift $w/\delta w$. Straight lines indicate best fit to power laws, $\alpha \sim w^{0.92}$, $\lambda \sim w^{1.9}$. Inset: Same as main figure, but for the delocalized frequency window of 10.5–12 GHz. As opposed to the main figure, here $\lambda \sim w^{1.0}$, in agreement with Eq. (4).

as fitting parameters. We have extracted α, λ, for various wall shifts w and plotted them versus a rescaled shift, $w/\delta w$. The results are summarized in Fig. 4. We find that in the frequency window 6–7.5 GHz (where Anderson localization is present), the best fit with Eq. (4) gives $\lambda \sim \lambda_w^{\gamma}$, with $\gamma = 1.9 \pm 0.05$. This result violates the theoretical expectation $\gamma \approx 1$ and constitutes a direct confirmation that the RMT result Eq. (4) is not applicable in the localized regime. At the same time, the best fit of the experimental scattering fidelity with the prediction of the BRM modeling (1) gives that $\alpha \sim \lambda_w^{\gamma}$ with $\gamma \sim 0.92 \pm 0.05$, in agreement with our theory. The extracted slope $\alpha/\lambda_w \sim \sqrt{I}2$ can be used as an estimation for the localization properties of our sample. Within the delocalized frequency window 10.5–12 GHz, a fit with Eq. (4) works perfectly well with $\gamma \approx 1.0 \pm 0.05$, in nice agreement with theory (see inset of Fig. 4). Here we meet the situation found for the fidelity decay observed in chaotic billiards when moving one wall [16].

In conclusion, using echo dynamics, we isolated absorption phenomena and identified traces of localization in random media. Our theory, based on a RMT modeling, indicated that the IPN of localized modes dictates the behavior of the LE which follows a novel decay law; being experimentally distinguishable from the Gaussian decay observed in diffusive or chaotic systems. Our experimental measurements with disordered waveguides confirm our theory, thus suggesting fidelity as a reliable tool to investigate localization in the presence of absorption.

The research was funded by the DFG FOR760 and by the US-Israel Binational Science Foundation (BSF), Jerusalem, Israel.

[1] P. Anderson, Phys. Rev. **109**, 1492 (1958).
[2] M. E. Gertsenshtein and V. B. Vasil'ev, Teor. Veroyatn. Primen. **4**, 391 (1959); **5**, 340(E) (1960).
[3] H. DeRaedt, A. Lagendijk, and P. deVries, Phys. Rev. Lett. **62**, 47 (1989).
[4] A. Chabanov, M. Stoytchev, and A. Genack, Nature (London) **404**, 850 (2000); A. A. Chabanov and A. Z. Genack, Phys. Rev. Lett. **87**, 233903 (2001); A. Genack and A. Chabanov, J. Phys. A **38**, 10 465 (2005).
[5] J. T. Edwards and D. J. Thouless, J. Phys. C **5**, 807 (1972).
[6] T. Gorin *et al.*, Phys. Rep. **435**, 33 (2006); Ph. Jacquod and C. Petitjean, Adv. Phys. **58**, 67 (2009).
[7] S. A. Gardiner, J. I. Cirac, and P. Zoller, Phys. Rev. Lett. **79**, 4790 (1997); M. F. Andersen, A. Kaplan, and N. Davidson, Phys. Rev. Lett. **90**, 023001 (2003); S. Kuhr *et al.*, Phys. Rev. Lett. **91**, 213002 (2003).
[8] R. Schäfer *et al.*, Phys. Rev. Lett. **95**, 184102 (2005).
[9] O. I. Lobkis and R. L. Weaver, Phys. Rev. Lett. **90**, 254302 (2003).
[10] M. A. Nielsen and I. L. Chuang, *Quantum Computation and Quantum Information* (Cambridge University Press, Cambridge, England, 2000).
[11] R. A. Jalabert and H. M. Pastawski, Phys. Rev. Lett. **86**, 2490 (2001); F. M. Cucchietti, C. H. Lewenkopf, E. R. Mucciolo, H. M. Pastawski, and R. O. Vallejos, Phys. Rev. E **65**, 046209 (2002).
[12] Ph. Jacquod, I. Adagideli, and C. W. J. Beenakker, Phys. Rev. Lett. **89**, 154103 (2002); Ph. Jacquod, I. Adagideli, and C. W. J. Beenakker, Europhys. Lett. **61**, 729 (2003).
[13] N. R. Cerruti and S. Tomsovic, Phys. Rev. Lett. **88**, 054103 (2002); J. Phys. A **36**, 3451 (2003).
[14] T. Gorin, T. Prosen, and T. H. Seligman, New J. Phys. **6**, 20 (2004); T. Prosen and M. Znidaric, J. Phys. A **35**, 1455 (2002); T. Kottos and D. Cohen, Europhys. Lett. **61**, 431 (2003); M. Hiller *et al.*, Phys. Rev. Lett. **92**, 010402 (2004).
[15] G. Benenti and G. Casati, Phys. Rev. E **65**, 066205 (2002); Y. Adamov, I. V. Gornyi, and A. D. Mirlin, Phys. Rev. E **67**, 056217 (2003); G. S. Ng, J. Bodyfelt, and T. Kottos, Phys. Rev. Lett. **97**, 256404 (2006).
[16] R. Schäfer *et al.*, New J. Phys. **7**, 152 (2005).
[17] H. U. Baranger and P. A. Mello, Phys. Rev. Lett. **73**, 142 (1994).
[18] A. Mirlin, R. Pnini, and B. Shapiro, Phys. Rev. E **57**, R6285 (1998); A. A. Chabanov and A. Z. Genack, *ibid.* **72**, 055602(R) (2005).
[19] G. Casati *et al.*, Phys. Rev. Lett. **72**, 2697 (1994); F. Izrailev *et al.*, Phys. Rev. E **55**, 4951 (1997).
[20] Y. V. Fyodorov and A. D. Mirlin, Int. J. Mod. Phys. B **8**, 3795 (1994).
[21] D. Cohen and T. Kottos, Phys. Rev. E **63**, 036203 (2001); M. Hiller, T. Kottos, and T. Geisel, Phys. Rev. A **73**, 061604(R) (2006).
[22] Y. V. Fyodorov, Phys. Rev. Lett. **73**, 2688 (1994); P. Kunstman, K. Zyczkowski, and J. Zakrzewski, Phys. Rev. E **55**, 2446 (1997).
[23] Y. V. Fyodorov and A. D. Mirlin, Phys. Rev. B **51**, 13403 (1995).

Probing Localization in Absorbing Systems via Loschmidt Echos

Bodyfelt, JD

2009-06-26